Available online at www.sciencedirect.com
SCIENCE DIRECT
Polymer 47 (2006) 3576–3582
polymer
www.elsevier.com/locate/polymer

Doped polyaniline/multi-walled carbon nanotube composites: Preparation, characterization and properties

Tzong-Ming Wu *, Yen-Wen Lin

Department of Materials Science and Engineering, National Chung Hsing University, 250 Kuo Kuang Road, Taichung 402, Taiwan, ROC

Received 15 June 2005; received in revised form 23 January 2006; accepted 18 March 2006

Abstract

This study reports the synthesis of doped polyaniline in its emeraldine salt form (PANI-ES) with carboxylic acid and acylchloride groups contained multi-walled carbon nanotubes (designated as c-MWNTs and a-MWNTs) by in situ polymerization. Both Raman spectra and HRTEM images indicate that carboxylic acid and acylchloride groups formed at both ends and on the sidewalls of the MWNTs. Based on the π–π* electron interaction between aniline monomers and functionalized MWNT and hydrogen bonding interaction between the amino groups of aniline monomers and the carboxylic acid/acylchloride groups of functionalized MWNT, aniline molecules were adsorbed and polymerized on the surface of MWNTs. Structural analysis by FESEM and HRTEM showed that PANI-ES/c-MWNT and PANI-ES/a-MWNT composites are core (c-MWNT or a-MWNT)- shell (doped-PANI-ES) tubular structures with diameters of several tens to hundreds of nanometers, depending on the PANI content. The conductivities of 0.5 wt% functionalized MWNT containing PANI-ES/c-MWNT and PANI-ES/a-MWNT composites are 60–70% higher than that of PANI without MWNT.
© 2006 Elsevier Ltd. All rights reserved.

Keywords: Carbon nanotubes; Polyaniline; Chemical treatment

1. Introduction

Carbon nanotubes (CNTs), discovered by Iijima et al. [1], have received much interest for their use in fabricating a new classes of advanced materials due to their unique structural, mechanical and electronic properties. They have potential for use in field emitters [2], probe tips for SPMs [3], nanoelectronic devices [4,5] and nanotube-based composites [6,7]. As expected for theoretical reasons, experimentally introducing CNTs into a polymer matrix improves the mechanical properties and electrical conductivity of the original polymer matrix [8–11]. Recent studies have shown that, besides possibly improving the mechanical and electrical properties of polymers, the formation of polymer/CNT composites is considered as a capable approach for an incorporation of CNTs into polymer-based devices [12–15]. Among these polymer/CNT composites, many reports have focused on the combination of CNT and conducting polymers including poly(3,4-ethylenedioxythiophene) (PEDOT)/CNT for forming a hole-conducting layer in organic light-emitting diodes [12] and poly(3-octylthiophene)/CNT [13] or poly(*p*-phenylene venylene) (PPV)/CNT [14] for use in highly efficient photovoltaic cells.

Among various conducting polymers, polyaniline (PANI) has a potential use in synthesizing polymer/CNT composites due to its good processability, environmental stability and reversible control of conductivity both by charge-transfer doping and protonation [16,17]. Significant progress has been made in fabricating PANI/CNT composite, with examples including PANI/multi-walled carbon nanotube (MWNT) composites that demonstrate site-selective interaction between the quinoid ring of the polymer and MWNT [18], the doped PANI/MWNT composite with or without protonic acid synthesized by in situ polymerization [19–22], coaxial nanowire of a PANI/MWNT composite prepared by electrochemical reaction [23] and the fabrication of PANI/single-walled carbon nanotube composites [24,25]. Although recent studies show a unique compatibility between PANI and CNT, the nature of PANI/CNT remains unclear.

This work describes the synthesis and characterization of protonic acid doped PANI with MWNTs fabricated by in situ polymerization. In order to improve the MWNT–PANI interface, chemical functionalization of the MWNT is used to

* Corresponding author. Tel.: +886 4 22840500x806; fax: +886 4 22857017.
E-mail address: tmwu@dragon.nchu.edu.tw (T.-M. Wu).

0032-3861/$ - see front matter © 2006 Elsevier Ltd. All rights reserved.
doi:10.1016/j.polymer.2006.03.060

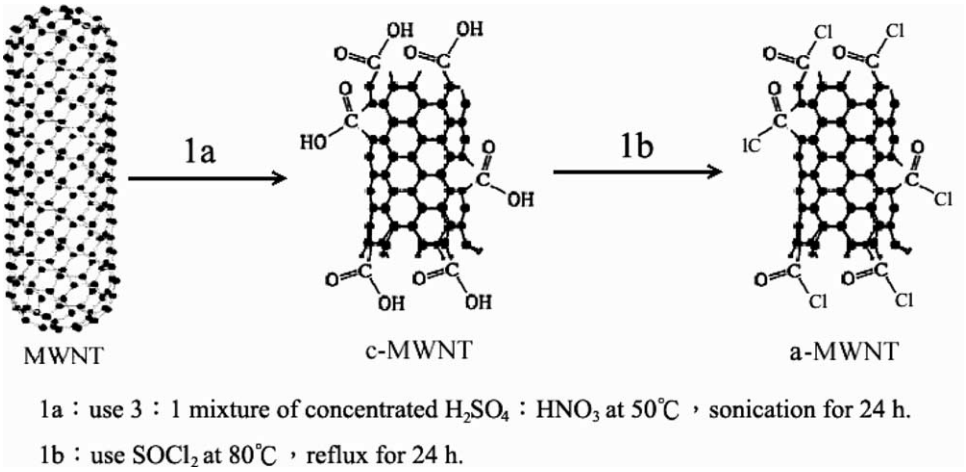

Fig. 1. Chemical routes for the preparation of functionalized MWNTs.

increase the interfacing binding between the MWNT and PANI. Functionalized nanotubes are also easier to disperse in organic solvent and water [26,27], which can improve the dispersion and homogeneity of the MWNTs within the polymer matrix. Therefore, the as-prepared MWNTs were first treated with a 3:1 mixture of concentrated H_2SO_4:HNO_3 [27], which produced carboxylic acid groups at the defect sites (designated as c-MWNT) and thus improved the solubility of the c-MWNTs in HCl solution. Then the carboxylic acid groups can be converted into acylchloride groups (designated as a-MWNTs) by the following treatment with $SOCl_2$ [28,29]. Corresponding chemical reactions are illustrated in Fig. 1. The interaction between aniline monomers and functionalized MWNTs is such that nanocomposites of doped-PANI with c-MWNTs or a-MWNTs can be synthesized by in situ chemical oxidation polymerization. To the best of our knowledge this is the first report of preparation of PANI/a-MWNT composites. The structure, morphology and conductivity of PANI/c-MWNT and PANI/a-MWNT composites were characterized: in particular, the tubular morphology was observed and the possible mechanism of the formation of this nanostructure was also discussed.

2. Experimental

2.1. Synthesis of PANI/c-MWNT and PANI/a-MWNT composites

The MWNTs used in this work were synthesized by ethylene CVD using Al_2O_3 supported Fe_2O_3 catalysts as described in a previous study [30]. The as-prepared MWNTs were ultrasonically treated with a 3:1 mixture of concentrated H_2SO_4 and HNO_3 at 50 °C for 24 h, which produced carboxylic acid groups at the defect sites and thus improved the solubility of the c-MWNTs in HCl solution. The c-MWNTs were then stirring with a mixture of $SOCl_2$ and *N*,*N*-ddimethyl formamide (DMF) at 80 °C for 24 h, which can be further converted the carboxylic acid at the defect sites into acylchloride group (a-MWNT). The a-MWNT was then filtered, rinsed several times with anhydrous THF, and died under a vacuum at 60 °C for 24 h.

The composite of protonic acid doped polyaniline (PANI) with c-MWNT or a-MWNT was synthesized by in situ chemical oxidation polymerization. In a typical synthesis experiment of PANI/c-MWNT composites, various weight ratio of c-MWNTs were dissolved in 1.0 M HCl solutions and ultrasonicated over 3 h, then transferred into a 500 ml four-neck flask with an ice-bath. Aniline monomer also dissolved in 1.0 M HCl solution was added to the above c-MWNTs suspension. For PANI/a-MWNT composites, various weight ratio of a-MWNTs were first mixed with aniline monomer and ultrasonicated over 3 h, then transferred into a 500 ml four-neck flask with an ice-bath. A 200 ml 1.0 M HCl solution containing 0.125 M Ammonium persulfate (APS) was slowly added dropwise into the suspension of both systems with constant mechanical stirring at a reaction temperature of 0–5 °C for 1 h. The reaction mixture was stirred for an additional 2 h at 0–5 °C, and then the resulting green suspension, indicating the formation of insoluble polyaniline in its emeraldine salt form (designated as PANI-ES), was then filtered and rinsed several times with distilled water and methanol. The powder obtained was dried under a vacuum at 60 °C for 24 h.

2.2. Structural analysis

The ATR-FTIR spectroscopy, UV–vis spectroscopy and Raman spectroscopy were used to characterize the structure of PANI-ES/c-MWNT and PANI-ES/a-MWNT composite. UV–vis spectra were performed on a Hitachi U-3010 with scanning speed at 200 nm/min and bandwidth 0.1 nm. The peak position of UV–vis spectra is determined using Peakfit software package. ATR-FTIR was recorded on a Pike Technologies ATR 6142, equipped with a ZnSe crystal. Samples in KBr were analyzed at room temperature without any dilution. Raman spectra were recorded under a Renishaw system 1000 using an Argon ion laser operating at 514.5 nm with a CCD detector. The final spectrum presented is an

average of three spectra recorded at different regions over the entire range of the sample. Thermal stabilities of these samples were operated using Perkin–Elmer thermogravimetric analysis (TGA). Linear $\theta/2\theta$ X-ray intensity scans of these specimens were recorded using a Mac MXT III diffractometer in the reflection mode, with Ni-filtered Cu Kα radiation.

2.3. Morphological analysis

The field-emission scanning electron microscopy (FESEM) and high-resolution transmission electron microscopy (HRTEM) were used to characterize the morphology of PANI-ES/c-MWNT and PANI-ES/a-MWNT composite. Ultra-thin section of the PANI-ES/c-MWNT and PANI-ES/a-MWNT sample with a thickness of approximate 50 nm was prepared with an ultramicrotome equipped with a diamond knife. FESEM was conducted at 3 kV using a JEOL JSM-6700F field-emission instrument and high-resolution transmission electron microscope (HRTEM) with selected area electronic diffraction images were recorded on a Hitachi HF-2000 at 200 kV. Due to the high electron density difference between carbon nanotube and polymer matrix, staining of the samples was not necessary.

2.4. Electrical properties

The samples of PANI, MWNT, PANI-ES/c-MWNT and PANI-ES/a-MWNT composites were pressed into pellet under 20 MPa. The conductivity at room temperature was measured by a programmable DC voltage/current detector (four probe method). Each data shown here is the mean value of the measurement from at least three samples.

3. Results and discussion

Fig. 2 shows the Raman spectrum of the MWNTs, c-MWNTs and a-MWNTS. All spectra have the same pattern, revealing that treating the surface with a 3:1 mixture of concentrated H_2SO_4:HNO_3 and then followed by the thionylchloride solution does not affect the graphite structure of the MWNTs. Such chemical functionalization of the MWNT can be used to produce carboxylic acid and acylchloride groups at local defects in the curved graphene sheets and tube ends. First-order Raman spectroscopy shows a strong band at 1580 cm^{-1} (G mode) which is the Raman-allowed phonon high-frequency mode and a disordered-induced peak at 1355 cm^{-1} (D mode), which may originate from the defects in the curved graphene sheets and tube ends. Comparing the I_G/I_D ratios of the samples, which are 1.72 for MWNTs and 1.58 for c-MWNTs, reveals the chemical functionalization of a mixture of concentrated H_2SO_4/HNO_3 increases the degree of disorder. The H_2SO_4/HNO_3 treated MWNTs is further modified by $SOCl_2$ to convert the carboxylic acid into acylchloride groups and the I_G/I_D ratio of a-MWNTs is decreased to 1.50, revealing the chemical treatment with $SOCl_2$ further increases the degree of disorder. Both results indicate the presence of defects at both the ends and the sidewalls of the c-MWNTs and a-MWNTs. Fig. 3 shows the ATR–FTIR spectrum of the MWNTs, c-MWNTs and a-MWNTs. The peak at around 1590 cm^{-1} corresponds to the IR active phonon mode of the MWNTs (Fig. 1, trace a) and the peaks at around 1730, 1170 and 1070 cm^{-1} apparently correspond to the stretching modes of the carboxylic acid groups (trace b in Fig. 1) [31]. The above results indicate the formation of carboxylic acid groups at both ends and on the sidewalls of the MWNTs. Besides a small peak at around 1710 cm^{-1} corresponds to the C=O stretching vibration of the COCl group (Fig. 1, trace c), the ATR-FTIR spectrum of the a-MWNTs did not show pronounced changes as compared to that of the c-MWNT samples. This is commonly a result of the poor quality of infrared spectra of MWNTs and the low concentration of organic moieties.

The thermogravimetric analysis was conducted to identify the thermal stability of MWNT, c-MWNTs and a-MWNTs. Fig. 4 shows the TGA thermal curves of the MWNTs, c-MWNTs and a-MWNTs. As seen from figure, the first weight loss below 100 °C is mainly attributed to loss of water molecules and lower molecular weight oligomers from the polymer matrix as suggested by earlier reports [32]. Then the steepest weight loss due to organic decomposition for the carboxylic acid and acylchloride groups is observed in a

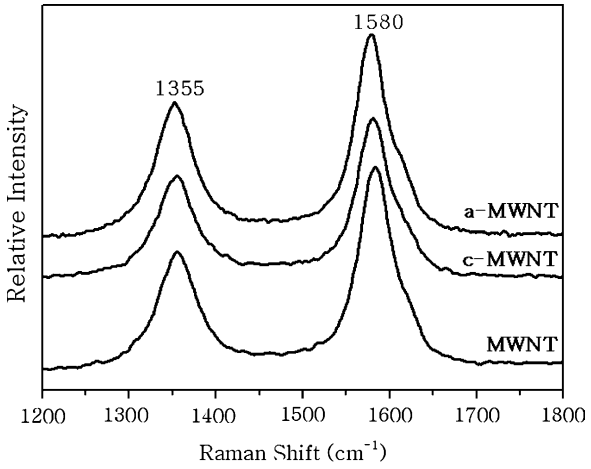

Fig. 2. Raman spectroscopy of MWNT, c-MWNT and a-MWNT.

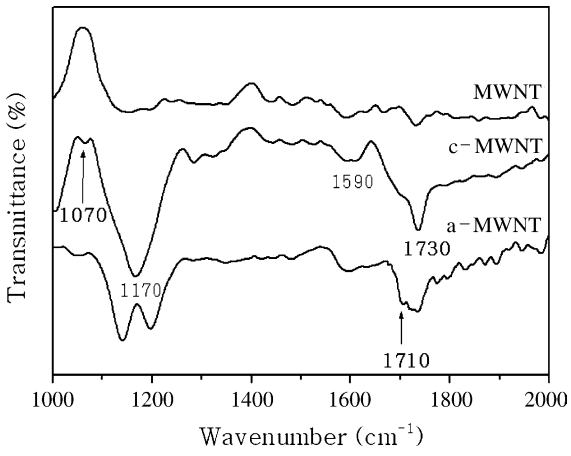

Fig. 3. FTIR spectroscopy of MWNT, c-MWNT and a-MWNT.

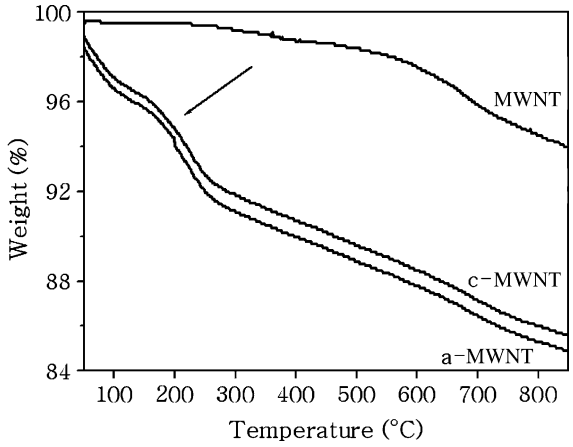

Fig. 4. Thermogravimetric curves of MWNT, c-MWNT and a-MWNT.

temperature interval of 100–250 °C, which may be due to the thermal degradation of the carboxylic acid and acylchloride groups formed at both ends and on the sidewalls of the MWNTs [33]. In order to investigate the surface of MWNTs, a direct observation of the functionalized MWNTs compared to untreated MWNTs was obtained by means of transmission electron microscopy. Fig. 5 presents the TEM image of the MWNTs, c-MWNTs and a-MWNTs. The sidewall of MWNT is very smooth, indicating the grapheme sheet fragments of the outer shell are relatively ordered. But the sidewalls of c-MWNT and a-MWNT are very rough and look like leaves that have been eaten by worms, these results may be explained by the electron beam destruction of the defect sites induced by the chemical functionalization. This result clearly reveals the multiple crystalline walls with surface defects and the hollow core of c-MWNT and a-MWNT, indicating the formation of carboxylic acid and acylchloride groups on the sidewalls. The corresponding electron diffraction pattern indicates that this MWNT has a crystalline structure.

The MWNT modified with carboxylic acid and acylchloride groups can be used as the self-assembly template for the formation of PANI nanostructures. The interaction between aniline monomers and functionalized MWNTs causes aniline molecules to be adsorbed on the surface of c-MWNTs and a-MWNTs. The protonic acid doped PANI/c-MWNT and PANI/a-MWNT composites are then synthesized successfully by in situ chemical oxidation polymerization. Fig. 6(a) presents the X-ray diffraction data for c-MWNT, PANI and PANI/c-MWNT composites. For c-MWNTs, the diffraction peaks at $2\theta = 25.9$ and 43° were observed, corresponding to graphite-like structure and small amounts of catalytic particles encapsulated inside the walls of CNTs, respectively [34]. Meanwhile, for PANI specimens, the crystalline peaks appeared at $2\theta = 9.4$, 15.3, 20.7, 25.2, 26.5 and 29.8°, corresponding to (001), (011), (020), (200), (121) and (022) reflections of polyaniline in its emeraldine salt form (designated as PANI-ES), respectively [35]. The X-ray data of PANI-ES/c-MWNT composites presents crystalline peaks similar to those obtained from the pure PANI matrix, revealing that no additional crystalline order had been introduced into the composites. The intensity ratio of the crystalline peaks for PANI-ES/c-MWNT composites is also close to that for pure PANI. This result indicates that even though there is a very thin amorphous layer on the surface of the c-MWNT, which is probably attributed to the irregular distribution of the COOH groups on the surface of c-MWNTs, and to the interaction between the quinoid ring of the polymer and c-MWNT. The c-MWNT further induces the packing of the PANI polymer chains along the axis of the c-MWNT and thus the percentage crystallinity of the outer layer of the PANI-ES/c-MWNT composites is almost the same as those of pure PANI molecules. The mass fraction of c-MWNT in PANI-ES/c-MWNT composites is sufficiently small that the graphite-like diffraction peaks can hardly be detected for 0.5 wt% MWNT-containing PANI-ES/c-MWNT composites. However, traces of diffraction peaks at $2\theta = 25.9°$ were observed as the ratio of c-MWNT increased to 3 wt%, indicating that part of the c-MWNT had not fully interacted with PANI molecules. The X-ray data of PANI-ES/a-MWNT composites with various content of a-MWNT shown in Fig. 6(b) shows similar tendency as those obtained from the PANI-ES/c-MWNT system, indicating that the further chemical treatment by $SOCl_2$ to form the acylchloride groups on the sidewall does not change their crystalline order of the composites.

To further confirm the nanostructure of PANI-ES/c-MWNT and PANI-ES/a-MWNT composites, typical FESEM and HRTEM images of the 3 wt% MWNT-containing PANI-ES/c-MWNT and PANI-ES/a-MWNT composites are shown in Fig. 7. For comparison, FESEM images of MWNT have also shown in this figure. For PANI-ES/c-MWNT composites, a tubular layer of a highly uniformly coated PANI film is clearly present on the c-MWNT surface and the diameters of the PANI-ES/c-MWNT composites range from several tens to hundreds of nanometers, depending on the PANI content

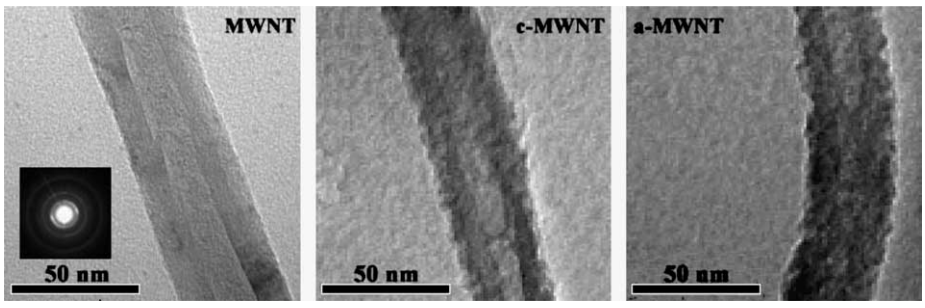

Fig. 5. HRTEM image of MWNT, c-MWNT and a-MWNT (inserted electron diffraction of MWNT).

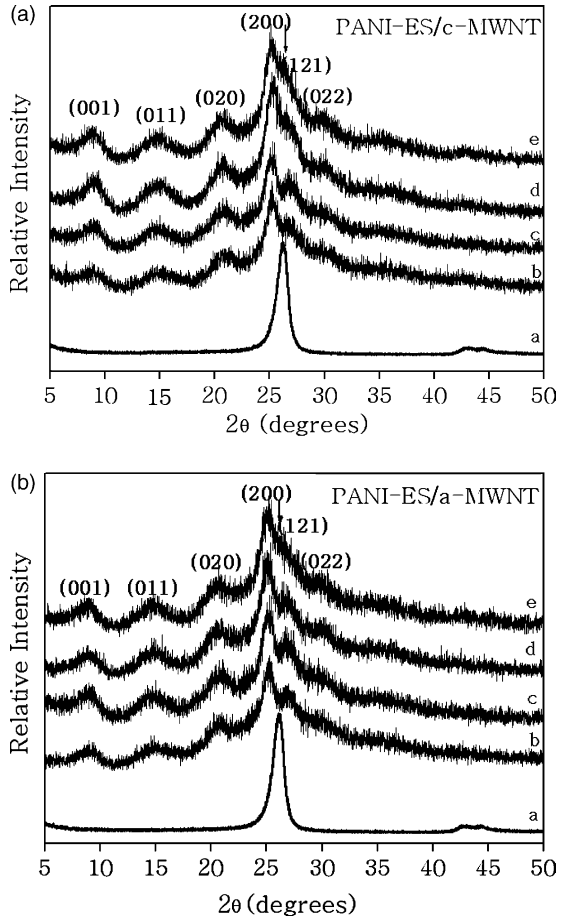

Fig. 6. (a) X-ray diffraction of (a) c-MWNT, (b) PANI-ES, (c) 0.5 wt% MWNT-contained PANI-ES/c-MWNT composite, (d) 1 wt% MWNT-contained PANI-ES/c-MWNT composite and (e) 3 wt% MWNT-contained PANI-ES/c-MWNT composite. (b) X-ray diffraction of (a) a-MWNT, (b) PANI-ES, (c) 0.5 wt% MWNT-contained PANI-ES/a-MWNT composite, (d) 1 wt% MWNT-contained PANI-ES/a-MWNT composite and (e) 3 wt% MWNT-contained PANI-ES/a-MWNT composite.

(Fig. 7(a)). The diameter of the PANI-ES/c-MWNT composites becomes larger than that of the original c-MWNTs after in situ polymerization. Closer inspection of HRTEM images (Fig. 7(c)) reveals that the resulting PANI-ES/c-MWNT composites have the coaxially tubular structures. The figures clearly show the hollow structure between the two sides of the multiple crystalline walls and the polyaniline macromolecules encapsulated at the surface of the c-MWNT (Fig. 7(c)). Similar morphology shown in Fig. 7(b) and (d) is also observed for PANI-ES/a-MWNT composites, but the resulting diameter is slightly larger than those observed for PANI-ES/c-MWNT composites. Nevertheless, both PANI-ES/c-MWNT and PANI-ES/a-MWNT composites are the typical core-shell structure, and the functionalized MWNTs serve as the core and are dispersed individually into the PANI matrices. The aniline monomer is uniformly polymerized on the surface of the MWNT and forms a tubular shell of fabricated composites. This tubular morphology is first reported for PANI/MWNT composites. Furthermore, the average thickness of the PANI layer ranges from several tens to hundreds of nanometers.

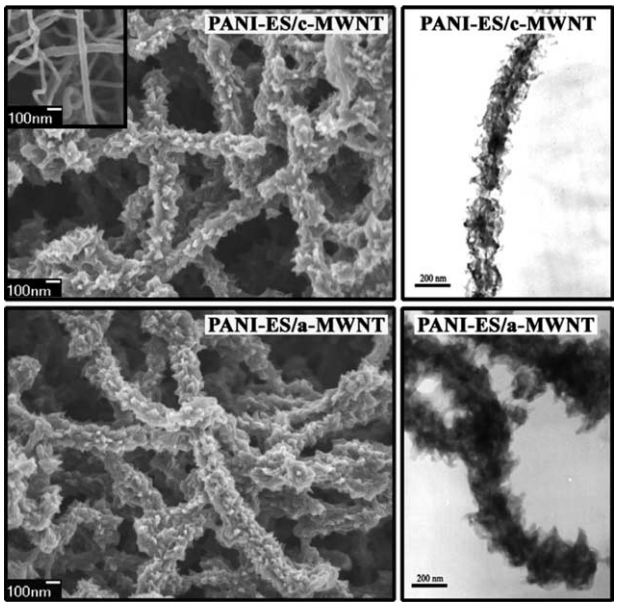

Fig. 7. FESEM and HRTEM images of 3 wt% MWNT-containing PANI-ES/c-MWNT and PANI-ES/a-MWNT composite (inserted FESEM of MWNT).

Fig. 8 shows the Raman spectra of PANI-ES/c-MWNT and PANI-ES/a-MWNT composites. For comparison, the figure also includes the spectrum of functionalized MWNTs, which contains two strong peaks at 1580 and 1355 cm^{-1}. For PANI-ES and PANI-ES/c-MWNT composites shown in Fig. 8(a), C–H bending of the quinoid ring at 1170 cm^{-1}, C–H bending of the benzenoid ring at 1260 cm^{-1}, $C–N^{+,\cdot}$ stretching at 1338 cm^{-1}, C=N stretching vibration at 1484 cm^{-1} and C–C stretching of the benzene ring at 1624 cm^{-1} were observed, revealing the presence of the doped PANI-ES structures [36,37]. Clearly, these Raman spectra are almost the same as those of PANI-ES and PANI-ES/c-MWNT composites, revealing that c-MWNT serves as the core in the formation of a tubular shell of PANI-ES/c-MWNT composites. Similar tendency is also observed for PANI-ES/a-MWNT system, which reveals that the further chemical functionalization by $SOCl_2$ to form the acylchloride groups on the sidewall does not change their core–shell tubular structures of the fabricated composites. It is necessary to point out the intensities of Raman peaks at 1170, 1338 and 1484 cm^{-1} corresponding to C–H bending of the quinoid ring, $C–N^{+,\cdot}$ and C=N stretching increase as the content of c-MWNT and a-MWNT increases. These results indicate more interaction between the quinoid ring of PANI-ES and functionalized MWNT as the content of c-MWNT and a-MWNT increases.

UV–vis spectroscopy was used to characterize the interfacial interaction between polymer and functionalized MWNT. Fig. 9(a) and (b) shows that the functionalized MWNT samples yield no absorption peaks in the range of 400–800 nm. The characteristic absorption peak of the sample of PANI-ES in *N*,*N*-dimethyl formamide (DMF) at approximately 450 nm is attributable to polaron–π transition on the polyemeraldine chain [38,39], indicating that the resulting PANI-ES is in the doped state. When the tubular nanostructure of fabricated

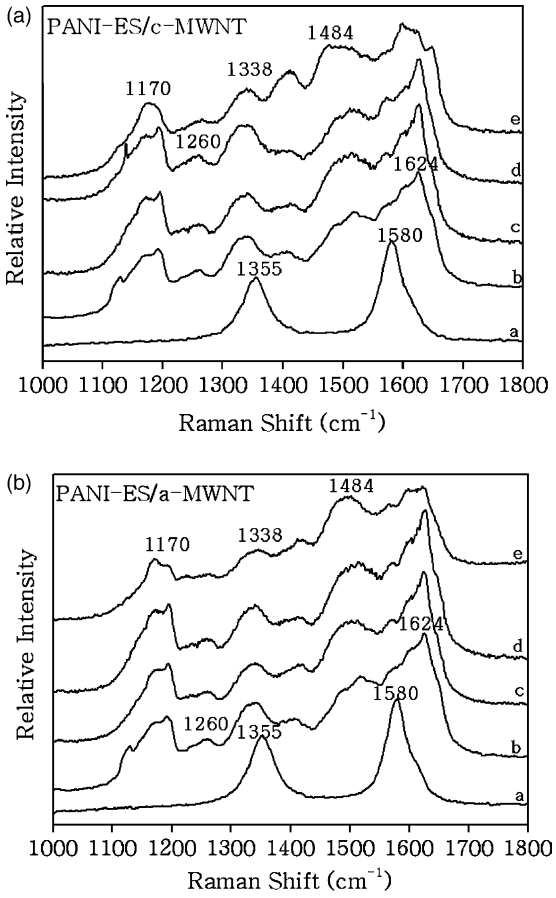

Fig. 8. (a) Raman spectroscopy of (a) c-MWNT, (b) PANI-ES, (c) 0.5 wt% MWNT-contained PANI-ES/c-MWNT composite, (d) 1 wt% MWNT-contained PANI-ES/c-MWNT composite and (e) 3 wt% MWNT-contained PANI-ES/c-MWNT composite. (b) Raman spectroscopy of (a) a-MWNT, (b) PANI-ES, (c) 0.5 wt% MWNT-contained PANI-ES/a-MWNT composite, (d) 1 wt% MWNT-contained PANI-ES/a-MWNT composite and (e) 3 wt% MWNT-contained PANI-ES/a-MWNT composite.

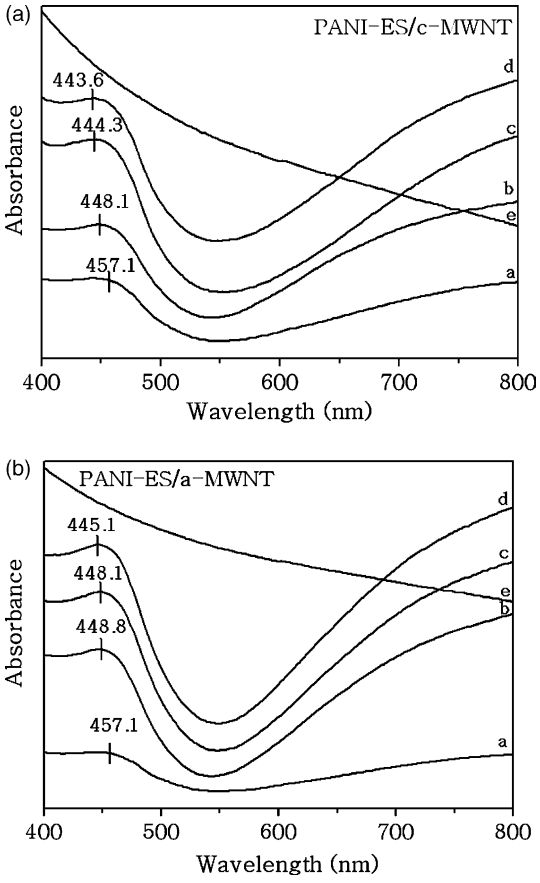

Fig. 9. (a) UV–vis spectroscopy of (a) PANI-ES, (b) 0.5 wt% MWNT-contained PANI-ES/c-MWNT composite, (c) 1 wt% MWNT-contained PANI-ES/c-MWNT composite and (d) 3 wt% MWNT-contained PANI-ES/c-MWNT composite and (e) c-MWNT. (b) UV–vis spectroscopy of (a) PANI-ES, (b) 0.5 wt% MWNT-contained PANI-ES/a-MWNT composite, (c) 1 wt% MWNT-contained PANI-ES/a-MWNT composite and (d) 3 wt% MWNT-contained PANI-ES/a-MWNT composite and (e) a-MWNT.

composites was formed, the characteristic peak assigned to the polaron–π transition on the polyemeraldine chain was slightly shifted to a smaller wavelength as the functionalized MWNT content increased, indicating the interaction between the quinoid ring of PANI-ES and functionalized MWNT [40]. These results are supported by the data observed from the images of HRTEM.

The formation mechanism of PANI-ES/c-MWNT and PANI-ES/a-MWNT composites with the tubular nanostructure is believed to involve strong interaction between aniline monomer and functionalized MWNT caused by the presence of the π–π* electron interaction between MWNT and the aniline monomer [34] as well as the hydrogen bond interaction between the carboxyl and acylchloride groups of functionalized MWNT and the amino groups of aniline monomers. Such strong interaction ensures that the aniline monomer is adsorbed on the surface of c-MWNTs or a-MWNTs, which serve as the core and self-assembly template during the formation of the tubular nanostructure. Although the surface of MWNT can be first treated with a mixture of concentrated H_2SO_4:HNO_3 and then further modified by the $SOCl_2$ to produce carboxylic acid and acylchloride groups at defect sites of c-MWNTs and a-MWNTs, and to increase the solubility of c-MWNTs and a-MWNTs in HCl solution, some functionalized MWNT bundles remain in a random conformation. Therefore, it is possible that there are some gaps between individual functionalized MWNT to allow the aniline molecules wriggle into such gaps and then in situ polymerization due to the strong π–π* electron/hydrogen bonding interaction between MWNTs and aniline monomers. The growing PANI polymer chain would possibly wedge away the MWNT bundles and then break down the bundles into individual MWNTs. In this case, functionalized MWNTs are uniformly and individually dispersed into PANI matrices. The site-selective interaction between the quinoid ring of the polymer and functionalized MWNT [20] causes PANI polymer chains to be adsorbed at the surface of the functionalized MWNT, which thus serves as the core of the tubular shell of PANI-ES/c-MWNT and PANI-ES/a-MWNT composites.

The electrical conductivities of PANI-ES, PANI-ES/c-MWNT and PANI-ES/a-MWNT composites were measured using the standard Van Der Pauw DC four-probe method [41]. The conductivities for functionalized MWNT and protonic

acid-doped PANI in its conductive emeraldine salt form at room temperature were 200 ± 3.4 and 29.6 ± 0.4 S/cm, respectively. As the addition of 0.5 wt% c-MWNT into PANI-ES, the conductivities at room temperature dramatically increase from 29.6 ± 0.4 to 48 ± 0.4 S/cm. With the continuous increase in the content of c-MWNT, the conductivities at room temperature gradually increase from 48 ± 0.4 S/cm for 0.5 wt% MWNT-containing PANI-ES/c-MWNT composites to 51.8 ± 0.4 and 58.4 ± 0.6 S/cm for 1 and 3 wt% MWNT-containing PANI-ES/c-MWNT composites, respectively. Such improvement is also obtained for PANI-ES/a-MWNT composites. The conductivity at room temperature increases from 29.6 ± 0.4 S/cm for PANI-ES to 51.3 ± 0.6, 55.2 ± 0.6 and 70.2 ± 0.8 S/cm for 0.5, 1 and 3 wt% MWNT-containing PANI-ES/a-MWNT composites, respectively. Comparing the conductivities with the same MWNT content at room temperature, reveals that the chemical functionalization of $SOCl_2$ increases the conductivities of composites. Nevertheless, the conductivities of fabricated composites with very low functionalized MWNT content at room temperature are more than 60–70% higher than those of PANI-ES without functionalized MWNT, perhaps because MWNTs have a large aspect ratio and surface area, and so may serve as a 'conducting bridge' between the PANI-ES conducting domains, increasing the effective path.

4. Conclusions

Both PANI-ES/c-MWNT and PANI/a-MWNT composites were prepared by the in situ polymerization. MWNTs that contained carboxylic acid and acylchloride groups were used as a core in the formation of tubular shells of PANI-ES/c-MWNT and PANI-ES/a-MWNT composites. Aniline molecules were adsorbed onto, and then polymerized on the surfaces of functionalized MWNTs. The electric conductivities at room temperature of 0.5 wt% functionalized MWNT containing PANI-ES/c-MWNT and PANI-ES/a-MWNT composites are about 60–70% higher than that of PANI without functionalized MWNT. That is because functionalized MWNT serves as a 'conducting bridge' between PANI-ES conducting domains, increasing the effective path.

Acknowledgements

The authors would like to thank the National Science Council for financially supporting this research under Contract No. NSC92-2622-E-005-006-CC3.

References

[1] Iijima S, Ichihashi T. Nature 1993;363:603.
[2] Fan S, Chapline MG, Franklin NR, Tombler TW. Science 1999;283:512.
[3] Dai H, Hafner JH, Rinzler AG, Colbert DT, Smalley RE. Nature 1996; 384:147.
[4] Frank S, Poncharal P, Wang ZL, de Heer WA. Science 1998;280:1744.
[5] Tans SJ, Verschueren ARM, Dekker C. Nature 1998;393:49.
[6] Ajayan PM, Stephan O, Colliex C, Trauth D. Science 1994;265:1212.
[7] Wong EW, Sheehan PE, Lieber CM. Science 1997;277:1971.
[8] Schadler LS, Giannaris SC, Ajayan PM. Appl Phys Lett 1998;73:3842.
[9] Qian D, Dickey EC, Andrews R, Rantell T. Appl Phys Lett 2000;76:2868.
[10] Baughman RH, Zakhidov AA, de Heer WA. Science 2002;297:787.
[11] Dai L, Mau AWH. Adv Mater 2001;13:899.
[12] Woo HS, Czerw R, Webster S, Carroll DL. Synth Met 2001;116:369.
[13] Kymakis E, Amaratunga GA. J Appl Phys Lett 2002;80:112.
[14] Ago H, Petritsch K, Shaffer MSP, Windle AH, Friend RH. Adv Mater 1999;11:1281.
[15] Curran SA, Ajayan PM, Blau WJ, Carroll DL. Adv Mater 1998;10:1091.
[16] Skotheim TA, Elsenbaumer RL, Reynolds JR. Handbook of conducting polymers. New York: Marcel Dekker; 1997.
[17] Premamoy G, Samir KS, Amit C. Eur Polym J 1999;35:699.
[18] Cochet M, Maser WK, Benito AM, Callejas MA. Chem Commun 2001; 40:1450.
[19] Deng JG, Ding XB, Zhang WC, Peng YX. Eur Polym J 2002;38:2497.
[20] Zengin H, Zhou W, Jin J, Czerw R, Smith DW. Adv Mater 2002;14:1480.
[21] Wei ZX, Wan MX, Lin T, Dai LM. Adv Mater 2003;15:136.
[22] Wu TM, Lin YW, Liao CS. Carbon 2005;43:734.
[23] Gao M, Huang SM, Dai LM, Wallace G. Angew Chem, Int Ed 2000;39: 3664.
[24] Blanchet GB, Fincher CR, Gao F. Appl Phys Lett 2003;82:1290.
[25] Li XH, Wu B, Huang JE, Zhang J. Carbon 2003;41:1670.
[26] Sun YP, Huang WJ, Lin Y, Fu KF, Kitaygorodskiy A, Riddle LA, et al. Chem Mater 2001;13:2864.
[27] Liu J, Rinzler AG, Dai HJ, Hafner JH, Bradley RK. Science 1998;280: 1253.
[28] Chen J, Hamon MA, Hu H, Chen Y, Rao AM, Eklund PC, et al. Science 1998;282:95.
[29] Hamon MA, Chen J, Hu H, Chen Y, Itkis ME, Rao AM, et al. Adv Mater 1999;11:834.
[30] Qian WZ, Wei F, Wang ZW, Liu T. AICHE J 2003;49:619.
[31] Mawhinney DB, Naumenko V, Kuznetsova A. J Am Chem Soc 2000;122: 2383.
[32] Gupta MC, Umare SS. Macromolecules 1992;25:138.
[33] Trchova M, Sedenkova I, Tobolkova E, Stejskal J. Polym Degrad Stab 2004;86:179.
[34] Liu SW, Yue J, Wehmschulte RJ. Nano Lett 2002;2:1439.
[35] Chaudhari HK, Kelkar DS. Polym Int 1997;42:380.
[36] Louarn G, Lapkowski M, Quillard S. J Phys Chem 1996;100:6998.
[37] Cochet M, Louarn G, Quillard S, Buisson JP, Lefrant S. J Raman Spectrosc 2000;31:1041.
[38] Dominis AJ, Spinks GM, Kane-Maguire LAP, Wallace GG. Synth Met 2002;129:165.
[39] Liu C, Zhang J, Shi G, Chen F. J Appl Polym Sci 2004;92:171.
[40] Xia H, Wang Q. J Appl Polym Sci 2003;87:1811.
[41] Van Der Pauw LJ. Philips Res Rep 1958;13:1.